

Search for the Electric Dipole Moment of the τ Lepton

Belle Collaboration

K. Inami^v, K. Abe^h, K. Abe^{al}, R. Abe^{aa}, T. Abe^{am},
 I. Adachi^h, H. Aihara^{an}, M. Akatsu^v, Y. Asano^{ar}, T. Aso^{aq},
 V. Aulchenko^b, T. Aushev^l, A. M. Bakich^{aj}, Y. Ban^{ae},
 E. Banas^y, P. K. Behera^{as}, I. Bizjak^m, A. Bondar^b,
 T. E. Browder^g, P. Chang^x, Y. Chao^x, B. G. Cheon^{ai},
 R. Chistov^l, Y. Choi^{ai}, Y. K. Choi^{ai}, L. Y. Dong^j,
 S. Eidelman^b, V. Eiges^l, Y. Enari^v, C. Fukunaga^{ap},
 N. Gabyshev^h, A. Garmash^{b,h}, T. Gershon^h, B. Golob^{s,m},
 C. Hagner^{at}, F. Handa^{am}, T. Hara^{ac}, H. Hayashii^w,
 M. Hazumi^h, I. Higuchi^{am}, T. Higuchi^{an}, T. Hokuue^v,
 Y. Hoshi^{al}, W.-S. Hou^x, H.-C. Huang^x, T. Igaki^v, T. Iijima^v,
 A. Ishikawa^v, H. Ishino^{ao}, R. Itoh^h, H. Iwasaki^h, H. K. Jang^{ah},
 J. H. Kang^{av}, J. S. Kang^o, N. Katayama^h, H. Kawai^{an},
 Y. Kawakami^v, N. Kawamura^a, T. Kawasaki^{aa}, H. Kichimi^h,
 H. O. Kim^{ai}, Hyunwoo Kim^o, J. H. Kim^{ai}, S. K. Kim^{ah},
 S. Korpar^{t,m}, P. Krokovny^b, R. Kulasiri^e, A. Kuzmin^b,
 Y.-J. Kwon^{av}, J. S. Lange^{f,af}, G. Leder^k, S. H. Lee^{ah}, J. Li^{ag},
 D. Liventsev^l, R.-S. Lu^x, J. MacNaughton^k, F. Mandl^k,
 T. Matsuishi^v, S. Matsumoto^d, T. Matsumoto^{ap}, W. Mitaroff^k,
 H. Miyake^{ac}, H. Miyata^{aa}, T. Nagamine^{am}, Y. Nagasakaⁱ,
 T. Nakadaira^{an}, E. Nakano^{ab}, M. Nakao^h, J. W. Nam^{ai},
 S. Nishida^p, T. Nozaki^h, S. Ogawa^{ak}, T. Ohshima^v,
 T. Okabe^v, S. Okunoⁿ, S. L. Olsen^g, W. Ostrowicz^y,
 H. Ozaki^h, P. Pakhlov^l, H. Park^q, K. S. Park^{ai}, L. S. Peak^{aj},
 J.-P. Perroud^r, L. E. Piilonen^{at}, K. Rybicki^y, H. Sagawa^h,
 S. Saitoh^h, Y. Sakai^h, M. Satapathy^{as}, O. Schneider^r,
 S. Semenov^l, K. Senyo^v, M. E. Sevior^u, H. Shibuya^{ak},
 B. Shwartz^b, V. Sidorov^b, J. B. Singh^{ad}, N. Soni^{ad},
 S. Stanič^{ar,1}, M. Starič^m, A. Sugi^v, A. Sugiyama^v,

K. Sumisawa^h, T. Sumiyoshi^{ap}, S. Suzuki^{au}, S. Y. Suzuki^h,
T. Takahashi^{ab}, F. Takasaki^h, K. Tamai^h, N. Tamura^{aa},
J. Tanaka^{an}, M. Tanaka^h, G. N. Taylor^u, Y. Teramoto^{ab},
S. Tokuda^v, T. Tomura^{an}, T. Tsuboyama^h, T. Tsukamoto^h,
S. Uehara^h, Y. Unno^c, S. Uno^h, G. Varner^g, K. E. Varvell^{aj},
C. C. Wang^x, Y. Watanabe^{ao}, B. D. Yabsley^{at}, Y. Yamada^h,
A. Yamaguchi^{am}, Y. Yamashita^z, Y. Yusa^{am}, Z. P. Zhang^{ag},
V. Zhilich^b, and D. Žontar^{s,m}

^a*Aomori University, Aomori, Japan*

^b*Budker Institute of Nuclear Physics, Novosibirsk, Russia*

^c*Chiba University, Chiba, Japan*

^d*Chuo University, Tokyo, Japan*

^e*University of Cincinnati, Cincinnati, OH, USA*

^f*University of Frankfurt, Frankfurt, Germany*

^g*University of Hawaii, Honolulu, HI, USA*

^h*High Energy Accelerator Research Organization (KEK), Tsukuba, Japan*

ⁱ*Hiroshima Institute of Technology, Hiroshima, Japan*

^j*Institute of High Energy Physics, Chinese Academy of Sciences, Beijing, PR China*

^k*Institute of High Energy Physics, Vienna, Austria*

^l*Institute for Theoretical and Experimental Physics, Moscow, Russia*

^m*J. Stefan Institute, Ljubljana, Slovenia*

ⁿ*Kanagawa University, Yokohama, Japan*

^o*Korea University, Seoul, South Korea*

^p*Kyoto University, Kyoto, Japan*

^q*Kyungpook National University, Taegu, South Korea*

^r*Institut de Physique des Hautes Énergies, Université de Lausanne, Lausanne, Switzerland*

^s*University of Ljubljana, Ljubljana, Slovenia*

^t*University of Maribor, Maribor, Slovenia*

^u*University of Melbourne, Victoria, Australia*

^v*Nagoya University, Nagoya, Japan*

^w*Nara Women's University, Nara, Japan*

^x*National Taiwan University, Taipei, Taiwan*

^y*H. Niewodniczanski Institute of Nuclear Physics, Krakow, Poland*

^z*Nihon Dental College, Niigata, Japan*

^{aa}*Niigata University, Niigata, Japan*
^{ab}*Osaka City University, Osaka, Japan*
^{ac}*Osaka University, Osaka, Japan*
^{ad}*Panjab University, Chandigarh, India*
^{ae}*Peking University, Beijing, PR China*
^{af}*RIKEN BNL Research Center, Brookhaven, NY, USA*
^{ag}*University of Science and Technology of China, Hefei, PR China*
^{ah}*Seoul National University, Seoul, South Korea*
^{ai}*Sungkyunkwan University, Suwon, South Korea*
^{aj}*University of Sydney, Sydney, NSW, Australia*
^{ak}*Toho University, Funabashi, Japan*
^{al}*Tohoku Gakuin University, Tagajo, Japan*
^{am}*Tohoku University, Sendai, Japan*
^{an}*University of Tokyo, Tokyo, Japan*
^{ao}*Tokyo Institute of Technology, Tokyo, Japan*
^{ap}*Tokyo Metropolitan University, Tokyo, Japan*
^{aq}*Toyama National College of Maritime Technology, Toyama, Japan*
^{ar}*University of Tsukuba, Tsukuba, Japan*
^{as}*Utkal University, Bhubaneswar, India*
^{at}*Virginia Polytechnic Institute and State University, Blacksburg, VA, USA*
^{au}*Yokkaichi University, Yokkaichi, Japan*
^{av}*Yonsei University, Seoul, South Korea*

Abstract

We have searched for a CP violation signature arising from an electric dipole moment (d_τ) of the τ lepton in the $e^+e^- \rightarrow \tau^+\tau^-$ reaction. Using an optimal observable method and 29.5 fb^{-1} of data collected with the Belle detector at the KEKB collider at $\sqrt{s} = 10.58 \text{ GeV}$, we find $Re(d_\tau) = (1.15 \pm 1.70) \times 10^{-17} e \text{ cm}$ and $Im(d_\tau) = (-0.83 \pm 0.86) \times 10^{-17} e \text{ cm}$ and set the 95% confidence level limits $-2.2 < Re(d_\tau) < 4.5 (10^{-17} e \text{ cm})$ and $-2.5 < Im(d_\tau) < 0.8 (10^{-17} e \text{ cm})$.

Key words: tau, electric dipole moment, CP violation, optimal observable
PACS: 13.40.Gp, 13.35.Dx, 14.60.Fg

¹ on leave from Nova Gorica Polytechnic, Nova Gorica, Slovenia

1 Introduction

While large CP violating asymmetry has recently been confirmed in B-meson decay [1,2], the Standard Model (SM) does not predict any appreciable CP violation (CPV) in the lepton sector. However, physics beyond the SM could produce CPV in leptonic processes; we would expect such effects to be enhanced for τ leptons due to their large mass. Parameterizing CPV in τ -pair production by an electric dipole moment d_τ , several authors have found possible effects of order $|d_\tau| \sim 10^{-19}e\text{ cm}$ due to new physics models [3,4]. The best existing bounds on d_τ are indirect, requiring $|d_\tau| < \mathcal{O}(10^{-17})e\text{ cm}$ based on naturalness arguments [5] and precision LEP data [6].² Previous direct measurements have been performed at LEP, where L3 [9] found $-3.1 < \text{Re}(d_\tau) < 3.1 \times 10^{-16}e\text{ cm}$ and OPAL [10] found $|\text{Re}(d_\tau)| < 3.7 \times 10^{-16}e\text{ cm}$, using the process $e^+e^- \rightarrow \tau^+\tau^-\gamma$; and by ARGUS [11], which set limits $|\text{Re}(d_\tau)| < 4.6 \times 10^{-16}e\text{ cm}$ and $|\text{Im}(d_\tau)| < 1.8 \times 10^{-16}e\text{ cm}$ based on a study of $e^+e^- \rightarrow \tau^+\tau^-$ production.

In this paper we present the first direct measurement of the τ lepton's electric dipole moment with a sensitivity in the $10^{-17}e\text{ cm}$ range. We improve on the sensitivity of ARGUS by an order of magnitude, by reducing the systematic uncertainty in the extraction of d_τ , and by analyzing a much larger sample of events.

We search for CP violating effects at the $\gamma\tau\tau$ vertex in the process $e^+e^- \rightarrow \gamma^* \rightarrow \tau^+\tau^-$ using triple momentum and spin correlation observables. The CP violating effective Lagrangian can be expressed as

$$\mathcal{L}_{CP} = -id_\tau(s)\bar{\tau}\sigma^{\mu\nu}\gamma_5\tau\partial_\mu A_\nu, \quad (1)$$

where the electric dipole form factor d_τ depends in general on s , the squared energy of the τ -pair system. In common with other authors, we ignore this possible s -dependence, assuming $d_\tau(s) \equiv d_\tau$, which is constant. ($d_\tau(0)$ corresponds to the electric dipole moment of the τ , and we shall use this term hereafter.) The squared spin density matrix ($\mathcal{M}_{\text{prod}}^2$) for τ -pair production $e^+(\mathbf{p})e^-(-\mathbf{p}) \rightarrow \tau^+(\mathbf{k}, \mathbf{S}_+)\tau^-(-\mathbf{k}, \mathbf{S}_-)$ is given by [12]

$$\begin{aligned} \mathcal{M}_{\text{prod}}^2 &= \mathcal{M}_{\text{SM}}^2 + \text{Re}(d_\tau)\mathcal{M}_{Re}^2 + \text{Im}(d_\tau)\mathcal{M}_{Im}^2 + |d_\tau|^2\mathcal{M}_{d^2}^2, \\ \mathcal{M}_{\text{SM}}^2 &= \frac{e^4}{k_0^2}[k_0^2 + m_\tau^2 + |\mathbf{k}^2|(\hat{\mathbf{k}} \cdot \hat{\mathbf{p}})^2 - \mathbf{S}_+ \cdot \mathbf{S}_- |\mathbf{k}|^2(1 - (\hat{\mathbf{k}} \cdot \hat{\mathbf{p}})^2)] \\ &\quad + 2(\hat{\mathbf{k}} \cdot \mathbf{S}_+)(\hat{\mathbf{k}} \cdot \mathbf{S}_-)(|\mathbf{k}|^2 + (k_0 - m_\tau)^2(\hat{\mathbf{k}} \cdot \hat{\mathbf{p}})^2) + 2k_0^2(\hat{\mathbf{p}} \cdot \mathbf{S}_+)(\hat{\mathbf{p}} \cdot \mathbf{S}_-) \end{aligned} \quad (2)$$

² A very strict constraint $|d_\tau| < 2.2 \times 10^{-25}e\text{ cm}$ has also been derived from the experimental limits on $\mu \rightarrow e\gamma$ decay [7]. We note, however, that this result assumes a particular ansatz for the lepton mixing matrix. In a recent preprint [8], other authors have argued that the same constraint may be derived under weaker assumptions.

$$-2k_0(k_0 - m_\tau)(\hat{\mathbf{k}} \cdot \hat{\mathbf{p}})((\hat{\mathbf{k}} \cdot \mathbf{S}_+)(\hat{\mathbf{p}} \cdot \mathbf{S}_-) + (\hat{\mathbf{k}} \cdot \mathbf{S}_-)(\hat{\mathbf{p}} \cdot \mathbf{S}_+)), \quad (3)$$

$$\mathcal{M}_{Re}^2 = 4 \frac{e^3}{k_0} |\mathbf{k}| [-(m_\tau + (k_0 - m_\tau)(\hat{\mathbf{k}} \cdot \hat{\mathbf{p}})^2)(\mathbf{S}_+ \times \mathbf{S}_-) \cdot \hat{\mathbf{k}} + k_0(\hat{\mathbf{k}} \cdot \hat{\mathbf{p}})(\mathbf{S}_+ \times \mathbf{S}_-) \cdot \hat{\mathbf{p}}], \quad (4)$$

$$\mathcal{M}_{Im}^2 = 4 \frac{e^3}{k_0} |\mathbf{k}| [-(m_\tau + (k_0 - m_\tau)(\hat{\mathbf{k}} \cdot \hat{\mathbf{p}})^2)(\mathbf{S}_+ - \mathbf{S}_-) \cdot \hat{\mathbf{k}} + k_0(\hat{\mathbf{k}} \cdot \hat{\mathbf{p}})(\mathbf{S}_+ - \mathbf{S}_-) \cdot \hat{\mathbf{p}}], \quad (5)$$

$$\mathcal{M}_{d^2}^2 = 4e^2 |\mathbf{k}|^2 \cdot (1 - (\hat{\mathbf{k}} \cdot \hat{\mathbf{p}})^2)(1 - \mathbf{S}_+ \cdot \mathbf{S}_-), \quad (6)$$

where k_0 is the energy of the τ , m_τ is the τ mass, \mathbf{p} is the momentum vector of e^+ , \mathbf{k} is the momentum vector of τ^+ in the center-of-mass frame, \mathbf{S}_\pm are the spin vectors for τ^\pm , and the hat denotes a unit momentum. We disregard the higher order terms proportional to $|d_\tau^2|$, which is valid since d_τ is small. \mathcal{M}_{SM}^2 corresponds to the SM term. \mathcal{M}_{Re}^2 and \mathcal{M}_{Im}^2 are the interference terms (related to the real and imaginary parts of d_τ , respectively) between the SM and CPV amplitudes. \mathcal{M}_{Re}^2 is CP odd and T odd, while \mathcal{M}_{Im}^2 is CP odd, but T even. In the above equations, e^+ and e^- are assumed to be unpolarized and massless particles.

We adapt the so-called optimal observable method [13], which maximizes the sensitivity to d_τ . Here the optimal observables are defined as

$$\mathcal{O}_{Re} = \frac{\mathcal{M}_{Re}^2}{\mathcal{M}_{SM}^2}, \quad \mathcal{O}_{Im} = \frac{\mathcal{M}_{Im}^2}{\mathcal{M}_{SM}^2}. \quad (7)$$

The mean value of the observable \mathcal{O}_{Re} is given by

$$\langle \mathcal{O}_{Re} \rangle \propto \int \mathcal{O}_{Re} \mathcal{M}_{prod}^2 d\phi = \int \mathcal{M}_{Re}^2 d\phi + Re(d_\tau) \int \frac{(\mathcal{M}_{Re}^2)^2}{\mathcal{M}_{SM}^2} d\phi, \quad (8)$$

where the integration is over the phase space (ϕ) spanned by the relevant kinematic variables. The cross-term containing the integral of the product of \mathcal{M}_{Re}^2 and \mathcal{M}_{Im}^2 drops out because of their different symmetry properties. The expression for the imaginary part is similar. The means of the observables $\langle \mathcal{O}_{Re} \rangle$ and $\langle \mathcal{O}_{Im} \rangle$ are therefore linear functions of d_τ ,

$$\langle \mathcal{O}_{Re} \rangle = a_{Re} \cdot Re(d_\tau) + b_{Re}, \quad \langle \mathcal{O}_{Im} \rangle = a_{Im} \cdot Im(d_\tau) + b_{Im}. \quad (9)$$

Eight different final states in the decay of τ -pairs, $(e\nu\bar{\nu})(\mu\nu\bar{\nu})$, $(e\nu\bar{\nu})(\pi\nu)$, $(\mu\nu\bar{\nu})(\pi\nu)$, $(e\nu\bar{\nu})(\rho\nu)$, $(\mu\nu\bar{\nu})(\rho\nu)$, $(\pi\nu)(\rho\nu)$, $(\rho\nu)(\rho\bar{\nu})$, and $(\pi\nu)(\pi\bar{\nu})$, are analyzed, where all particles except ν and $\bar{\nu}$ are positively or negatively charged. Because of the undetectable particles, we can not fully reconstruct the quantities \mathbf{k} and \mathbf{S}_\pm . Therefore, for each event we calculate possible kinematic configurations and obtain the mean value of \mathcal{M}_{SM}^2 , \mathcal{M}_{Re}^2 and \mathcal{M}_{Im}^2 by averaging over the calculated configurations. In the case when both τ leptons decay hadronically ($\tau \rightarrow \pi\nu$ or $\rho\nu$), the τ flight direction is calculated with a two-fold ambiguity [14] and we take the average of \mathcal{M}_{SM}^2 , \mathcal{M}_{Re}^2 and \mathcal{M}_{Im}^2 over the two solutions. In the case when either one or both τ leptons decay

leptonically ($\tau \rightarrow e\nu\bar{\nu}$ or $\mu\nu\bar{\nu}$), a Monte Carlo (MC) treatment is adopted to take into account the additional ambiguity in the effective mass of the $\nu\bar{\nu}$ system ($m_{\nu\bar{\nu}}$). For each event we generate 100 MC configurations using a hit-and-miss approach by varying $m_{\nu\bar{\nu}}$, and compute the averaged $\mathcal{M}_{\text{SM}}^2$, \mathcal{M}_{Re}^2 and \mathcal{M}_{Im}^2 over successful tries in which the τ direction can be constructed kinematically. In the calculation, we ignore the effect of undetected photons coming from initial state radiation, radiative τ decays and bremsstrahlung. The resulting bias in d_τ is included among the systematic errors; the effect on the final result is negligible.

2 Data and event selection

In this analysis, we use 26.8 million τ -pairs (29.5 fb^{-1}) accumulated with the Belle detector [15] at the KEKB accelerator [16]. KEKB is an asymmetric energy e^+e^- collider with a beam crossing angle of 22 mrad. Its center-of-mass energy is 10.58 GeV, corresponding to the $\Upsilon(4S)$ resonance, with beam energies of 8 and 3.5 GeV for electrons and positrons, respectively. Belle is a general-purpose detector with an asymmetric structure along the beam direction. Among the detector elements, the central drift chamber (CDC) and the silicon vertex detector (SVD) are essential to obtain the momentum vectors of charged particles. The combined information from the silica Aerogel Cherenkov counters (ACC), the time-of-flight counters (TOF), the CsI electromagnetic calorimeter (ECL), and the μ/K_L detector (KLM) is used for particle identification.

The MC event generators KORALB/TAUOLA [17] are used for τ -pair production and decays. The detector simulation is performed with a GEANT-based program, GSIM. Actual data and MC generated events are reconstructed by the same program written by the Belle collaboration.

We reconstruct the eight τ -pair decay modes mentioned above, with the following conditions. Each charged track is required to have a transverse momentum $p_t > 0.1 \text{ GeV}/c$. Photon candidates should deposit an energy of $E > 0.1 \text{ GeV}$ in the ECL. A signal event is required to have two charged tracks with zero net-charge and no photon apart from $\rho^\pm \rightarrow \pi^\pm\pi^0$, $\pi^0 \rightarrow \gamma\gamma$.

A track is identified as an electron using a likelihood ratio combining dE/dx in the CDC, the ratio of energy deposited in the ECL and momentum measured in the CDC, the shower shape in the ECL and the hit pattern from the ACC. The identification efficiency is estimated to be 92% with a π^\pm fake rate of 0.3% for the momentum range between $1.0 \text{ GeV}/c$ and $3.0 \text{ GeV}/c$ in the laboratory frame [18]. A muon is identified by its range and hit pattern in the KLM detector, with efficiency and fake rate estimated to be 91% and 2%,

Table 1

Yield, purity and background rate obtained for the event selection described in the text, where the purity is evaluated by MC simulation and its error comes from MC statistics.

	Yield	Purity (%)	Background mode (%)
$e\mu$	250,948	96.6 ± 0.1	$2\gamma \rightarrow \mu\mu(1.9)$, $\tau\tau \rightarrow e\pi(1.1)$.
$e\pi$	132,574	82.5 ± 0.1	$\tau\tau \rightarrow e\rho(6.0)$, $eK(5.4)$, $e\mu(3.1)$, $eK^*(1.3)$.
$\mu\pi$	123,520	80.6 ± 0.1	$\tau\tau \rightarrow \mu\rho(5.7)$, $\mu K(5.3)$, $\mu\mu(2.9)$, $2\gamma \rightarrow \mu\mu(2.0)$.
$e\rho$	240,501	92.4 ± 0.1	$\tau\tau \rightarrow e\pi\pi^0\pi^0(4.4)$, $eK^*(1.7)$.
$\mu\rho$	217,156	91.6 ± 0.1	$\tau\tau \rightarrow \mu\pi\pi^0\pi^0(4.2)$, $\mu K^*(1.6)$, $\pi\rho(1.0)$.
$\pi\rho$	110,414	77.7 ± 0.1	$\tau\tau \rightarrow \rho\rho(5.1)$, $K\rho(4.9)$, $\pi\pi\pi^0\pi^0(3.8)$, $\mu\rho(2.7)$.
$\rho\rho$	93,016	86.2 ± 0.1	$\tau\tau \rightarrow \rho\pi\pi^0\pi^0(8.0)$, $\rho K^*(3.1)$.
$\pi\pi$	28,348	70.0 ± 0.2	$\tau\tau \rightarrow \pi\rho(9.2)$, $\pi K(9.2)$, $\pi\mu(4.7)$, $\pi K^*(2.0)$.

respectively, for momenta in the laboratory frame greater than $1.2 \text{ GeV}/c$. A track is considered to be a pion if it is identified as a hadron by the KLM information and not identified as an electron: the efficiency of this selection is estimated to be 81%, and the purity for the selected samples is estimated by MC to be 89%. A ρ^\pm is reconstructed from a charged track and a π^0 where the track should be neither an electron nor a muon, and for $\pi^0 \rightarrow \gamma\gamma$, the reconstructed π^0 should have an invariant mass between 110 and 150 MeV/c^2 and a momentum in the laboratory frame larger than $0.2 \text{ GeV}/c$. In order to suppress background and to improve the performance of the particle identification cuts, we restrict the analysis to lepton candidates within the barrel region, $-0.60 < \cos\theta < 0.83$, and to pion candidates for $\tau \rightarrow \pi\nu$ within the KLM barrel region, $-0.50 < \cos\theta < 0.62$, where θ is the polar angle opposite to the e^+ beam direction in the laboratory frame. For the same reason, the laboratory frame particle momentum is required to be greater than $0.5 \text{ GeV}/c$ for an electron, $1.2 \text{ GeV}/c$ for both a muon and pion, and $1.0 \text{ GeV}/c$ for the ρ^\pm .

The dominant backgrounds are due to two-photon as well as Bhabha and $\mu\mu$ processes. In order to remove two-photon events, we require the missing momentum not to be directed towards the beam-pipe region (imposing a selection $-0.950 < \cos\theta < 0.985$), and to reject the latter processes we require that the sum of the charged track momenta be less than $9 \text{ GeV}/c$ in the center-of-mass frame. Additional selections are imposed particularly on the $e\pi$ mode where a large number of Bhabha events could contribute through misidentification. For the $e\pi$ mode, we remove events which satisfy the following criteria: the opening angle of the two tracks in the plane perpendicular to the beam axis is greater than 175° , and their momentum sum is greater than $6 \text{ GeV}/c$ in the τ -pair rest frame. Finally, we remove events in which the τ flight direction cannot be kinematically reconstructed, which mostly arise from τ -pairs having

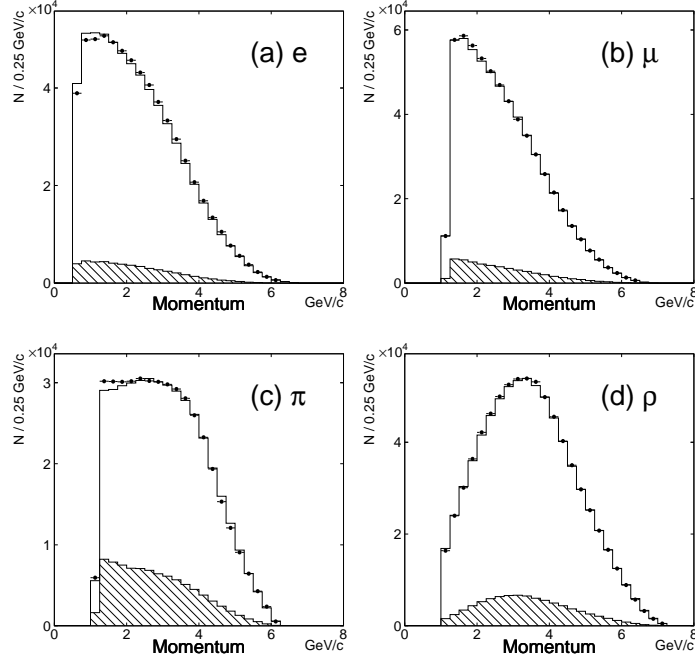


Fig. 1. Momentum distributions of (a) e^\pm , (b) μ^\pm , (c) π^\pm , and (d) ρ^\pm in the laboratory frame. The points with error bars are the data and the histogram is the MC expectation. The latter is scaled to the total number of entries. The hatched histogram is the background distribution evaluated by MC.

hard initial-state radiation and misidentified τ -pair backgrounds.

The yield of events passing this selection is given in Table 1 for each of the eight selected modes. The mean energy of the τ -pair system in the obtained sample is $\sqrt{s} = 10.38$ GeV; this sets the scale at which $d_\tau(s)$ is measured. Because of events with soft radiated photons, the energy scale is slightly lower than the beam energy. The dominant background sources are also listed in the table. Hadronic τ decays with two or more π^0 's make a contribution of a few percent. For the modes including π^\pm , kaons and misidentified muons from other τ decays produce a feed-across background; for example, we estimate that 5.3% of the $\mu\pi$ sample consists of μK decays. The other backgrounds are estimated by MC to be a few percent from two-photon processes, and less than 1% from Bhabha, $\mu\mu$, and multihadronic processes.

Figures 1 and 2 show the resulting momentum and $\cos\theta$ distributions, respectively, for charged particles in the laboratory frame. Very good agreement with MC is found, except for low-momentum electrons (Fig. 1(a)) and pions (Fig. 1(c)). The dip in the $\cos\theta$ distribution of the muon (Fig. 2(b)) is due to an efficiency drop at the region of overlap between the barrel and endcap KLM elements.

The resulting \mathcal{O}_{Re} and \mathcal{O}_{Im} distributions are shown in Fig. 3 along with those obtained from MC simulation with $d_\tau = 0$. Good agreement is found between

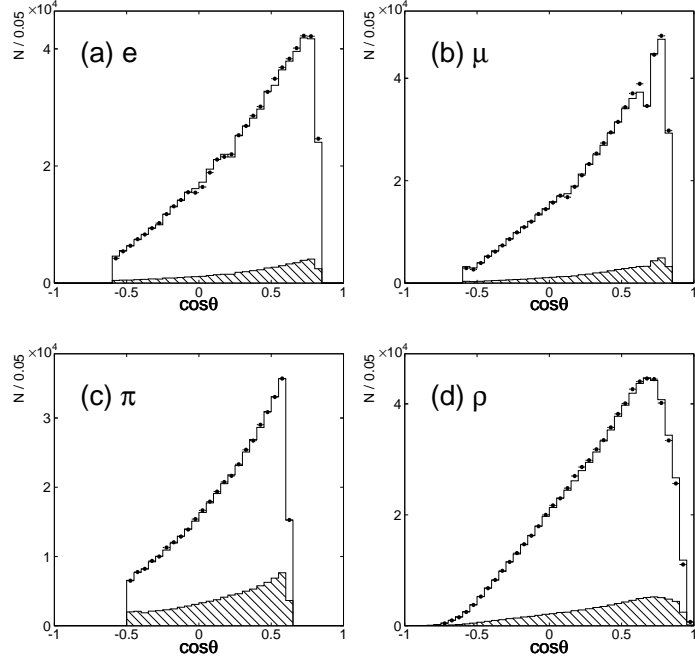


Fig. 2. The $\cos \theta$ distributions of (a) e^\pm , (b) μ^\pm , (c) π^\pm , and (d) ρ^\pm in the laboratory frame. The meanings of the points and histograms are the same as in Fig. 1.

the experimental data and the MC samples. Distributions of the ratio of the data to MC (not shown here) are flat and near 1.0.

3 Extraction of d_τ

In order to extract the d_τ value from the observable using Eq. (9), we have to know the coefficient a and the offset b . In the ARGUS analysis [11], which also used the optimal observable method, the first term of Eq. (8) was assumed to be negligible because it vanishes when the integration takes place over the full phase space: $\int \mathcal{M}_{Re}^2 d\phi = 0$. The value of d_τ was obtained as the ratio of the observable's mean to the second term, $Re(d_\tau) = \langle \mathcal{O}_{Re} \rangle / \langle \mathcal{O}_{Re}^2 \rangle$. However, the detector acceptance η affects the means of the observables according to

$$\langle \mathcal{O}_{Re} \rangle \propto \int \eta(\phi) \mathcal{O}_{Re} \mathcal{M}_{prod}^2 d\phi. \quad (10)$$

Similar expressions obtain for the imaginary part. This means that the first term of Eq. (8) is not necessarily zero and the coefficient may differ from $\langle \mathcal{O}_{Re}^2 \rangle$ when the detector acceptance is taken into account. In the ARGUS study, the acceptance effect produced the largest systematic uncertainty, of the order of $10^{-16} e \text{ cm}$.

In order to reduce this systematic effect, we extract both parameters a and

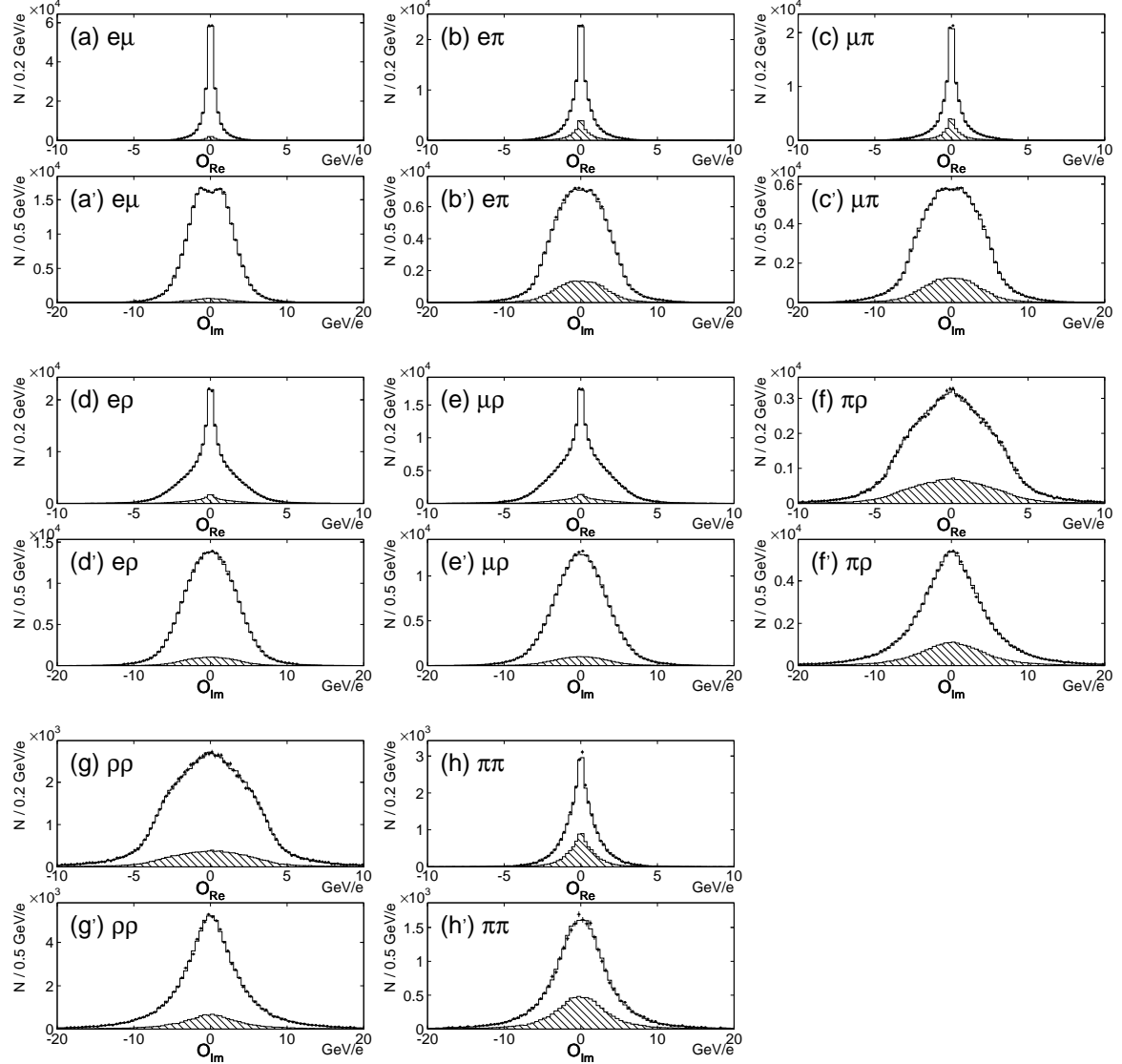


Fig. 3. Distributions of the optimal observables \mathcal{O}_{Re} and \mathcal{O}_{Im} for each mode. The upper figure of each mode is for \mathcal{O}_{Re} and lower figure is for \mathcal{O}_{Im} . The closed circles are the experimental data and the histogram is the MC expectation with $d_\tau = 0$, normalized to the number of entries. The hatched histogram is the background distribution evaluated by MC.

b from the correlation between $\langle \mathcal{O}_{Re} \rangle (\langle \mathcal{O}_{Im} \rangle)$ and $Re(d_\tau)(Im(d_\tau))$ obtained by a full MC including acceptance effects. An example of the correlation between $\langle \mathcal{O}_{Re} \rangle (\langle \mathcal{O}_{Im} \rangle)$ and $Re(d_\tau)(Im(d_\tau))$ is shown in Fig. 4. Each point is obtained from MC with detector simulation and event selection. By fitting the correlation plot with Eq. (9), the parameters a and b are obtained. The feed-across background from other τ decays shows some dependence on d_τ , because the spin direction is correlated with the momenta of the final state particles. Therefore, the effects of the feed-across background on the coefficient a and offset b are corrected using the parameters obtained from the background. The resulting coefficients and offsets are shown in Fig. 5.

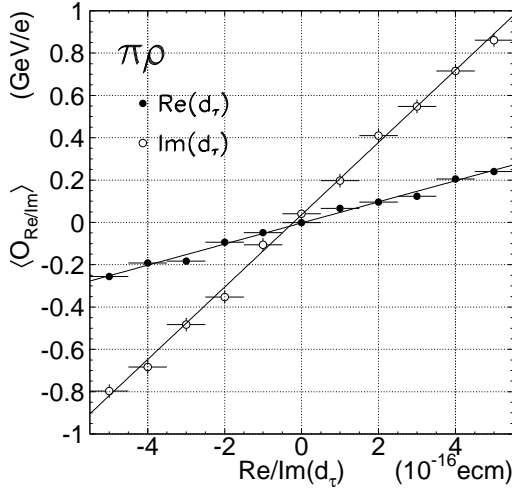


Fig. 4. $Re(d_\tau)$ ($Im(d_\tau)$) dependence of the mean of the observable $\langle \mathcal{O}_{Re} \rangle$ ($\langle \mathcal{O}_{Im} \rangle$) for the $\pi\rho$ mode. The closed circles show the dependence for $Re(d_\tau)$ and the open circles show the dependence for $Im(d_\tau)$. The lines show the fitted linear functions.

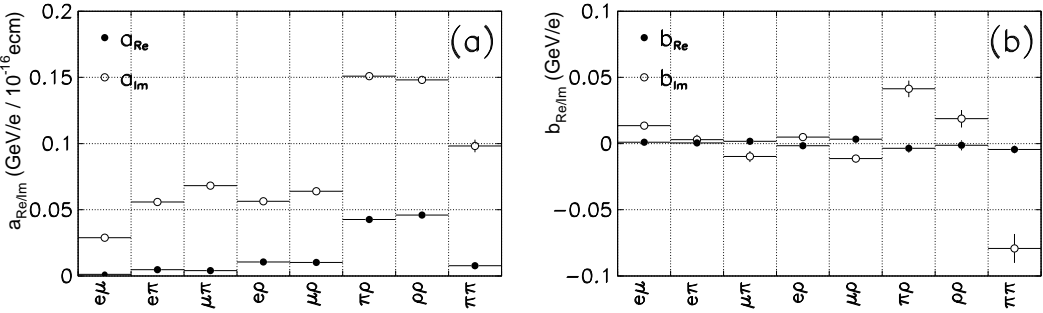


Fig. 5. Sensitivity a (a) and offset b (b) for each mode from MC. The closed circles show the parameters for $Re(d_\tau)$ and the open circles show the parameters for $Im(d_\tau)$. The errors are due to MC statistics.

As can be seen from the values of the coefficient a , the $\pi\rho$ and $\rho\rho$ modes have the highest sensitivities for d_τ , while the $\pi\pi$ mode has a somewhat lower sensitivity. For the real part, this is an effect of averaging over the two solutions for the τ direction: in the $\tau \rightarrow \pi\nu$ case, this causes spin correlation information to be lost, whereas for $\tau \rightarrow \rho\nu$ the angular distribution of the $\rho \rightarrow \pi\pi^0$ decay provides information on the τ spin which survives the averaging procedure. For the imaginary part, the lower sensitivity is due to the tighter $\cos\theta$ cut applied to pions in the $\tau \rightarrow \pi\nu$ channel, compared to $\tau \rightarrow \rho\nu$; there is also a small effect from the tighter momentum cut. The remaining modes, which include leptons, have low sensitivities because information about the τ spin, and also its direction, is lost due to the additional neutrino(s). Non-zero offsets b_{Im} are seen for the imaginary part, due to the forward/backward asymmetry in the acceptance of the detector.

4 Systematic uncertainties

Although in general the MC simulation reproduces the observed kinematic distributions well, the small disagreement that is evident in Figures 1 and 2 dominates the systematic uncertainty. The effect on d_τ is studied by reweighting the MC distributions by the ratio of data and MC. The second significant uncertainty originates from possible charge asymmetry in the detection efficiency. The ratio of yields, $N(\alpha^+\beta^-)/N(\alpha^-\beta^+)$, for data and MC agrees within 1%, where α and β are the relevant charged particles from the τ decays. The resulting systematic uncertainty is evaluated by varying the detection efficiency by $\pm 1\%$. The effect is of the same size as the statistical error for $Im(d_\tau)$, while it is negligible for $Re(d_\tau)$. The backgrounds lead to additional systematic uncertainties in d_τ because the parameters a and b are corrected for the background distributions: this effect is assessed by varying the assumed background rate. The effects of photon energy resolution, and of possible biases in reconstructed momentum (for charged tracks and photons), are checked by applying scaling factors based on a comparison of data and MC distributions. In order to examine a possible asymmetry arising from the alignment of the tracking devices, we measure the differences in polar angles, $\Delta\theta = \theta_{CM}^+ - \theta_{CM}^-$, and azimuthal angles, $\Delta\phi = \phi_{CM}^+ - \phi_{CM}^-$, for the two tracks in $e^+e^- \rightarrow \mu^+\mu^-$ events, and find a small deviation from back-to-back topological alignment in each direction: $\Delta\theta = 1.48$ mrad and $\Delta\phi = 0.36$ mrad. Applying an artificial angular deviation of this magnitude to one of the charged tracks, we find the change in the observables to be negligible compared to the other errors.

To estimate the effect of ignoring radiative processes in the calculation of the observables, we consider the case $d_\tau = 0$ and compare our standard calculation to one which includes initial state radiation, taking the shift in d_τ as a measure of the systematic error. Since this shift occurs in analysis of both data and MC events, it is already taken into account in the analysis (up to effects of detector and/or background mismodelling), so the estimate is conservative. For all decay modes apart from $\pi\pi$, the shift is negligibly small.

The various sources of systematic error are listed in Table 2.

5 Result

The values of d_τ extracted using Eq. (9) are listed in Table 3 along with the corresponding statistical and systematic errors, and plotted in Fig. 6. The results are consistent with $d_\tau = 0$ within the errors.

Finally, we obtain mean values for $Re(d_\tau)$ and $Im(d_\tau)$ over the eight different

Table 2
Systematic errors for $Re(d_\tau)$ and $Im(d_\tau)$ in units of $10^{-16}e\text{cm}$.

$Re(d_\tau)$	$e\mu$	$e\pi$	$\mu\pi$	$e\rho$	$\mu\rho$	$\pi\rho$	$\rho\rho$	$\pi\pi$
Mismatch of distribution	0.80	0.58	0.70	0.11	0.15	0.21	0.16	0.06
Charge asymmetry	0.00	0.01	0.01	0.01	0.01	0.01	-	-
Background variation	0.43	0.12	0.07	0.07	0.08	0.03	0.04	0.05
Momentum reconstruction	0.16	0.09	0.24	0.04	0.06	0.06	0.04	0.45
Detector alignment	0.02	0.02	0.01	0.00	0.01	0.01	0.02	0.03
Radiative effects	0.09	0.04	0.02	0.01	0.01	0.02	0.00	0.16
Total	0.93	0.60	0.74	0.14	0.18	0.22	0.17	0.48

$Im(d_\tau)$	$e\mu$	$e\pi$	$\mu\pi$	$e\rho$	$\mu\rho$	$\pi\rho$	$\rho\rho$	$\pi\pi$
Mismatch of distribution	0.43	0.02	0.05	0.12	0.01	0.05	0.10	0.41
Charge asymmetry	0.13	0.44	0.43	0.02	0.09	0.15	-	-
Background variation	0.08	0.07	0.02	0.01	0.03	0.02	0.03	0.06
Momentum reconstruction	0.03	0.03	0.06	0.00	0.02	0.02	0.04	0.04
Detector alignment	0.01	0.03	0.02	0.01	0.01	0.02	0.01	0.05
Radiative effects	0.05	0.02	0.01	0.01	0.01	0.02	0.01	0.02
Total	0.46	0.45	0.44	0.13	0.10	0.16	0.11	0.42

Table 3
Results for the electric dipole moment. The first error is statistical and the second is systematic.

Mode	$Re(d_\tau)$ ($10^{-16}e\text{cm}$)	$Im(d_\tau)$ ($10^{-16}e\text{cm}$)
$e\mu$	$2.25 \pm 1.26 \pm 0.93$	$-0.41 \pm 0.22 \pm 0.46$
$e\pi$	$0.43 \pm 0.64 \pm 0.60$	$-0.22 \pm 0.19 \pm 0.45$
$\mu\pi$	$-0.41 \pm 0.87 \pm 0.74$	$0.15 \pm 0.19 \pm 0.44$
$e\rho$	$0.00 \pm 0.36 \pm 0.14$	$-0.01 \pm 0.14 \pm 0.13$
$\mu\rho$	$0.04 \pm 0.42 \pm 0.18$	$-0.02 \pm 0.14 \pm 0.10$
$\pi\rho$	$0.34 \pm 0.25 \pm 0.22$	$-0.22 \pm 0.13 \pm 0.16$
$\rho\rho$	$-0.08 \pm 0.25 \pm 0.17$	$-0.12 \pm 0.14 \pm 0.11$
$\pi\pi$	$0.42 \pm 1.17 \pm 0.48$	$0.24 \pm 0.34 \pm 0.42$
Mean value	0.115 ± 0.170	-0.083 ± 0.086

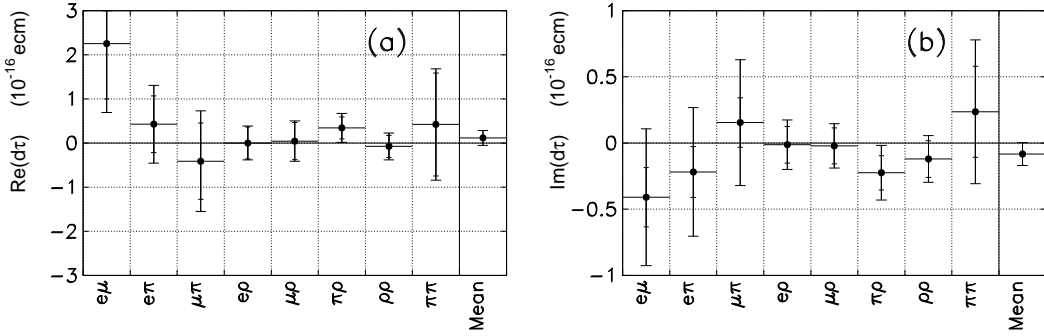


Fig. 6. $Re(d_\tau)$ and $Im(d_\tau)$ for each mode. Both statistical and systematic errors are included. The small ticks on the error bars show the statistical errors.

$\tau^+\tau^-$ modes weighted by quadratically summed statistical and systematic errors,

$$Re(d_\tau) = (1.15 \pm 1.70) \times 10^{-17} e \text{ cm}, \quad (11)$$

$$Im(d_\tau) = (-0.83 \pm 0.86) \times 10^{-17} e \text{ cm}, \quad (12)$$

with corresponding 95% confidence limits

$$-2.2 < Re(d_\tau) < 4.5 \quad (10^{-17} e \text{ cm}), \quad (13)$$

$$-2.5 < Im(d_\tau) < 0.8 \quad (10^{-17} e \text{ cm}). \quad (14)$$

This investigation has improved the sensitivity to the τ lepton's electric dipole moment by an order of magnitude over previous measurements.

Acknowledgements

We would like to thank Professors K. Hagiwara, O. Nachtmann, and Z. Wąs for their constructive advice and many helpful discussions. We also wish to thank the KEKB accelerator group for the excellent operation of the KEKB accelerator. We gratefully acknowledge the support from the Ministry of Education, Culture, Sports, Science, and Technology of Japan, Grant-in-Aid for JSPS Fellows 01655 2001, and the Japan Society for the Promotion of Science; the Australian Research Council and the Australian Department of Industry, Science and Resources; the National Science Foundation of China under contract No. 10175071; the Department of Science and Technology of India; the BK21 program of the Ministry of Education of Korea and the CHEP SRC program of the Korea Science and Engineering Foundation; the Polish State Committee for Scientific Research under contract No. 2P03B 17017; the Ministry of Science and Technology of the Russian Federation; the Ministry of Education, Science and Sport of the Republic of Slovenia; the National Science Council and the Ministry of Education of Taiwan; and the U.S. Department of Energy.

References

- [1] K. Abe et al. (Belle Collaboration), Phys. Rev. Lett. 87 (2001) 091802; Phys. Rev. D 66 (2002) 032007.
- [2] B. Aubert et al. (BaBar Collaboration), Phys. Rev. Lett. 87 (2001) 091801; Phys. Rev. D 66 (2002) 032003.
- [3] T. Huang, W. Lu, and Z. Tao, Phys. Rev. D 55 (1997) 1643.
- [4] W. Bernreuther, A. Brandenburg, and P. Overmann, Phys. Lett. B 391 (1997) 413; *ibid.*, B 412 (1997) 425.
- [5] K. Akama, T. Hattori, and K. Katsuura, Phys. Rev. Lett. 88 (2002) 201601.
- [6] R. Escribano and E. Massó, Phys. Lett. B 301 (1993) 419; Nucl. Phys. B 429 (1994) 19; Phys. Lett. B 395 (1997) 369.
- [7] T. Huang, Z. H. Lin, and X. Zhang, Phys. Lett. B 450 (1999) 257.
- [8] J. Q. Zhang, X. C. Song, W. J. Huo, and T. F. Feng, hep-ph/0205309.
- [9] M. Acciarri et al. (L3 Collaboration), Phys. Lett. B 434 (1998) 169.
- [10] K. Ackerstaff et al. (OPAL Collaboration), Phys. Lett. B 431 (1998) 188.
- [11] H. Albrecht et al. (ARGUS Collaboration), Phys. Lett. B 485 (2000) 37.
- [12] W. Bernreuther, O. Nachtmann, and P. Overmann, Phys. Rev. D 48 (1993) 78.
- [13] D. Atwood and A. Soni, Phys. Rev. D 45 (1992) 2405.
- [14] K. Ackerstaff et al. (OPAL Collaboration), Z. Phys. C 74 (1997) 403.
- [15] A. Abashian et al. (Belle Collaboration), Nucl. Instr. and Meth. A 479 (2002) 117.
- [16] E. Kikutani ed., KEK Preprint 2001-157 (2001), to appear in Nucl. Instr. and Meth. A.
- [17] KORALB(v.2.4)/TAUOLA(v.2.6): S. Jadach and Z. Wąs, Comp. Phys. Commun. 85 (1995) 453; *ibid.*, 64 (1991) 267; *ibid.*, 36 (1985) 191; S. Jadach, Z. Wąs, R. Decker, and J.H. Kühn, Comp. Phys. Commun. 64 (1991) 275; *ibid.*, 70 (1992) 69; *ibid.*, 76 (1993) 361.
- [18] K. Hanagaki et al., Nucl. Instr. and Meth. A 485 (2002) 490.